Fermi-LAT Study of Cosmic-rays/Diffuse Gamma-rays and Implications on Particle Physics

Tsunefumi MIZUNO[1] on behalf of the *Fermi*-LAT collaboration

[1]*Department of Physics, Hiroshima University, Hiroshima 739-8526, Japan*

The Galactic and extragalactic diffuse gamma-ray emission has been one of hot topics in high-energy astrophysics. The Galactic diffuse gamma-rays is a powerful probe to study cosmic-rays and the interstellar medium in the Milky Way. The extragalactic diffuse gamma-ray emission is composed of contributions from unresolved sources such as active galactic nuclei. They may also contain the signature of exotic physics like the annihilation of dark matter. Our knowledge of the diffuse gamma-ray emission was not good enough in the last century, however, due to the limited angular resolution, effective area and energy coverage of past instruments. The situation has been improved significantly by the advent of the Large Area Telescope (LAT) on board *Fermi* Gamma-ray Space Telescope launched in 2008 June. The *Fermi*-LAT also has a capability to measure cosmic-ray electron spectrum up to about 1 TeV and may probe nearby cosmic-ray electron accelerators or dark matter signal. We review the observation and analysis of the diffuse gamma-ray emission and cosmic-ray electrons by the *Fermi*-LAT, and implications on astrophysics and particle physics.

§1. Introduction

The Galactic diffuse gamma-ray emission is produced by interaction of Galactic cosmic-rays (CRs) with the interstellar medium (ISM) via nucleon-nucleon interaction and bremsstrahlung, and with the interstellar radiation field via inverse Compton scattering. It is a direct probe of Galactic CRs in distant locations, and may include signature of physics beyond the standard model, such as dark matter annihilation. Therefore the Galactic diffuse gamma-ray emission has been of significant interest and studied extensively since the beginning of the gamma-ray astrophysics.[1)–3)] It is also a foreground for the much fainter extragalactic diffuse emission.

One of the outstanding questions since the last century is a so-called "GeV-excess", the excess diffuse emission above 1 GeV seen in the EGRET data[4),5)] relative to that expected from the model based on the directly measured CR spectra. This finding led to the proposal that the emission was a long-awaited signature of dark matter annihilation.[6)] More conservative interpretations include the unexpectedly large variations of CR spectra in the Milky Way[7)] and the instrumental effect.[4)] The *Fermi*-LAT, with much improved sensitivity[8)] over the EGRET, had been expected to shed light on this issue.

The extragalactic diffuse gamma-ray emission, or the extragalactic gamma-ray background (EGB), was first detected by SAS-2 mission[9)] and its spectrum was measured up to 10 GeV by the EGRET.[10)] The EGRET also established that the blazars (active galactic nuclei with a relativistic jet pointing towards us) represent the most numerous populations of gamma-ray objects. Therefore, undetected blazars (i.e., those under the sensitivity level of EGRET) are the most likely candidates for the origin of the EGB. Studies of the luminosity function of blazars showed that the contribution of blazars to the EGRET EGB could be in the range of 20–100%.[11)–13)] It is thus possible that the EGB encrypts the signature of truly diffuse emission processes, such as intergalactic shocks produced by large-scale structures[14)] and the annihilation of dark matter. The contribution from non-blazar objects such as galaxy clusters and starburst/normal galaxies is also of interest. Therefore the EGB is one of main topics to be explored by the *Fermi*-LAT.

CR electrons lose energy rapidly via synchrotron radiation and inverse Compton scattering during their propagation in the interstellar space, making their spectrum softer than that of CR protons. This fact indicates that at the very high energy end CR electrons can probe nearby CR sources in the vicinity of the solar system. Recent results on the CR electron spectrum, published in 2008–2009 by PAMELA,[15] ATIC[16] and H.E.S.S.[17] have opened a new phase in the study of high-energy CR electrons. PAMELA reports an increase of positron fraction above 10 GeV, while ATIC detected a prominent spectral feature at around 500 GeV in the inclusive electron and positron spectrum. H.E.S.S. reports a sharp steepening or cutoff in the $e^- + e^+$ spectrum above 1 TeV. These results are not compatible with the conventional model of CR electrons and positrons proposed before. The nature of possible sources had been widely discussed, such as nearby pulsars and dark matter annihilation. (For a review, see Ref. 18))

§2. Galactic Diffuse Gamma-ray Emission

2.1. *Diffuse Gamma-rays at Intermediate Latitude*

Testing the GeV excess was one of the early studies of the diffuse gamma-ray emission seen by *Fermi*-LAT. Ref. 19) studied the data at intermediate Galactic latitude ($10° \leq |b| \leq 20°$). This region was chosen since it maximizes the fraction of signal from diffuse gamma-rays produced in the vicinity of the solar system, and hence uncertainties associated with CR propagation and knowledge of the ISM gas distribution should be minimized.

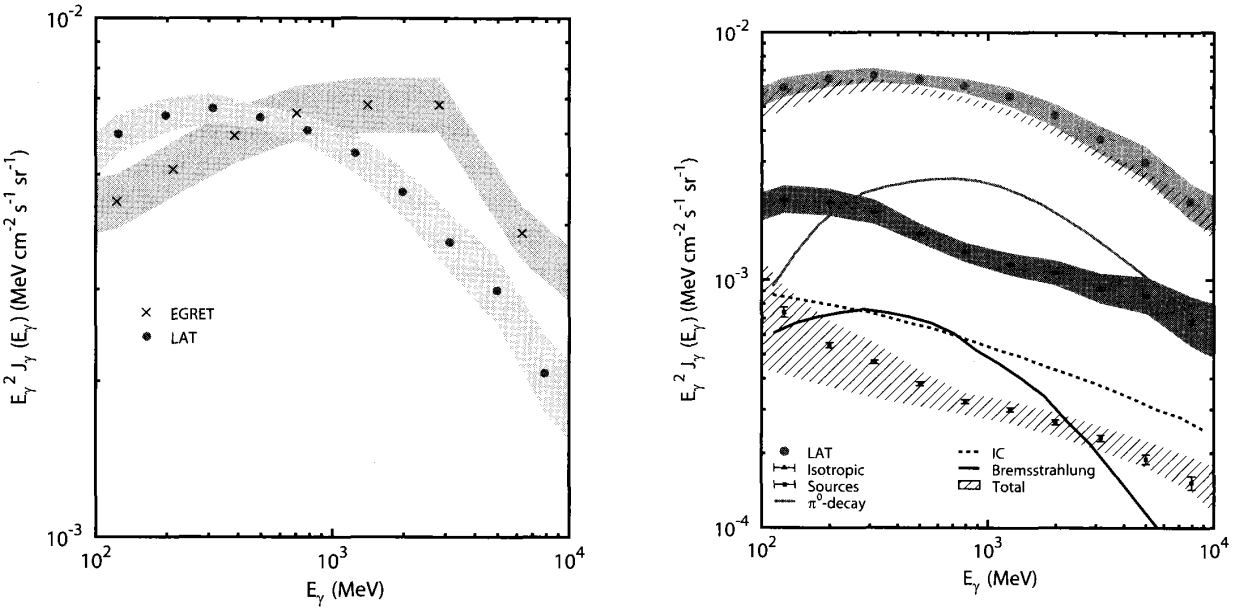

Fig. 1. (left) Diffuse emission spectra averaged over all Galactic longitudes for latitude range $10° \leq |b| \leq 20°$ obtained by the *Fermi* LAT[19] and the EGRET. Systematic uncertainties are shown by hatched areas. (right) *Fermi*-LAT data and the model for the same sky region. The contribution of each model component is also presented. Upper solid line and lower one represent the pion-decay and bremsstrahlung, respectively.

Figure 1 (left) shows LAT data averaged over all Galactic longitudes and latitude range $10° \leq |b| \leq 20°$. Also shown are the EGRET data for the same region of the sky. The hatched bands surrounding the LAT and EGRET represent the systematic uncertainties of these instruments. Although the contribution by point sources has not been subtracted for both data sets, the effect

on the diffuse emission is minor.

As shown by the figure, the LAT-measured spectrum is significantly softer than the EGRET measurement with an integrated intensity $J_{\rm LAT}(\geq 1\ {\rm GeV}) = (2.35 \pm 0.01) \times 10^{-6}\ {\rm cm}^{-2}\ {\rm s}^{-1}\ {\rm sr}^{-1}$ compared to the EGRET intensity $J_{\rm EGRET}(\geq 1\ {\rm GeV}) = (3.16 \pm 0.05) \times 10^{-6}\ {\rm cm}^{-2}\ {\rm s}^{-1}\ {\rm sr}^{-1}$ where the errors are statistical only. Even if we take account of the systematic uncertainties of two instruments, the LAT spectrum is lower and softer than that measured by the EGRET above 1 GeV. We thus do not confirm the EGRET GeV-excess in this region of the sky and give strong constraints on the dark matter interpretations proposed to explain the EGRET data.

On the other hand, the LAT spectrum agrees reasonably with the spectrum of an *a priori* diffuse gamma-ray model based on the pre-*Fermi* CR measurements as shown by the right panel of the figure. In this figure we replots the *Fermi*-LAT data along with the spectra of a diffuse emission model based on local CR measurements, sources detected with more than 5σ significance and an isotropic component. The last term is thought to be comprised of residual particle contamination and the true extragalactic diffuse emission, and was obtained by fitting to data at higher Galactic latitudes. The *Fermi*-LAT spectral shape agrees well with the model in 100 MeV – 10 GeV. Although the overall intensity of the model is systematically lower by 10–20%, the diffuse gamma-ray emission model is based on pre-*Fermi* data, and the difference between the model and the data is of the same order as the uncertainty in the measured CR spectra at the relevant energies. The uncertainty of the ISM gas distribution could also contribute to the observed small discrepancy. We thus conclude that the LAT data and the model agree well with each other, providing a solid basis for future work to understand the diffuse gamma-rays and the CR distribution in larger scale. We also note that, although the *Fermi*-LAT data rule out the large EGRET GeV-excess, it is still interesting to look for a smaller excess in diffuse gamma-ray emission from, e.g., the Galactic halo where the signal due to dark matter annihilation is expected.

2.2. *CR density Distribution*

Knowledge of the distribution of CR densities within our Galaxy is a key to understand their origin and propagation. We thus performed the analysis of diffuse gamma-ray emission observed in the second (Galactic longitude $100^\circ \leq l \leq 145^\circ$) and the third ($210^\circ \leq l \leq 250^\circ$) Galactic quadrants. Those windows host kinematically well-defined segments of the Galactic spiral arms present along the line of sight and are the best regions to study the CR density distribution across the outer Galaxy.

Following a well-established approach that dates back to the COS-B era,[20] we modeled the γ-ray emission as a linear combination of maps tracing the column density of the interstellar gas. Provided that the H I column densities are accurately measured, the emissivity per H I atom (traced by the 21 cm line of atomic hydrogen[21]) directly probes the average CR densities in each of the region studied. In Figure 2 we summarize the integrated emissivity gradient (above 200 MeV) found beyond the Solar circle in the second and the third quadrants. The bow-ties indicate the systematic uncertainty due to the optical depth correction applied to the H I line intensities, which was found to be the dominant source of the systematics. See Ref. 23),24) for details of the analysis. Despite the uncertainties due to the optical-depth correction, both LAT studies consistently point to a slowly decreasing emissivity profile beyond Galactocentric radius $R = 10$ kpc.

We will consider the predictions by a CR propagation model to see the impact of such a flat profile on the CR source distribution and propagation parameters. We utilize the GALPROP code,[25] a numerical code which solves the CR transport within the Galaxy. A conventional model with the CR halo size $z_{\rm h} = 4$ kpc predicts a gradient (solid line in Figure 2 left) steeper than that inferred from the LAT data.

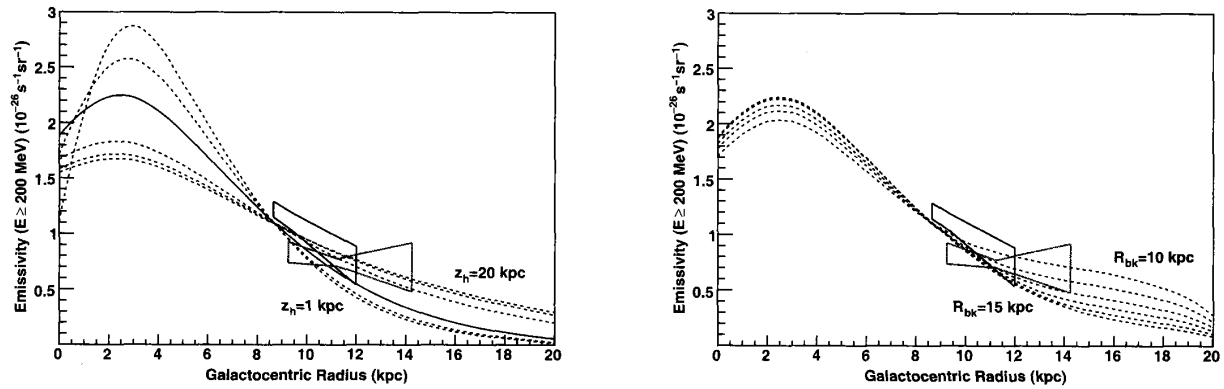

Fig. 2. Comparisons of the emissivity gradient obtained by the LAT and model expectations taken from Ref. 22). The bow-ties represent our estimates for the second (black) and the third (gray) quadrants, and the curves give the model predictions. The left panel shows models with different halo size from 1 kpc to 20 kpc (the solid line corresponds to 4 kpc). The right panel shows different choices of the break distance $R_{\rm bk}$ (from 10 to 15 kpc) beyond which a flat CR source distribution is assumed.

The discrepancy between the gamma-ray emissivity gradient and the distribution of putative CR sources has been known as the "gradient problem" since the COS-B era.[26] The most straightforward possibility is a larger halo size, as discussed by, e.g., Ref. 25)–27). We therefore tried several choices of $z_{\rm h}$ as summarized in the dotted lines in the same panel, and found that a very large halo ($z_{\rm h} \geq 10$ kpc) provides a gradient compatible with the gamma-ray data, if we fully take into account the systematic uncertainties. A CR source distributions flatter than a standard one are also investigated, as shown by the right panel of the figure. We obtained a reasonable fit to the data using a flat CR source distribution beyond $R = 10$ kpc. The LAT data thus favors a very large halo size and/or a flat CR source distribution than usually assumed.

Obviously the solution discussed above is not unique. The exploration could be extended to a non-uniform diffusion coefficient[28] or convection.[29] The bottom line is that the LAT data give good constraints on the CR and the matter distribution in the outer Galaxy and the diffuse gamma-ray model is significantly improved. In the future, the extension to the inner part and the accurate determination of the gradient over the whole Galaxy will be key to constraining the CR origin and transport. In addition, better modeling the Galactic diffuse emission is essential in searching for a dark matter signal in gamma-rays. For a review, see Ref. 30).

§3. Extragalactic Gamma-ray Background

The Galactic diffuse gamma-ray emission presents a strong foreground signal to the much fainter extragalactic diffuse emission, and hence is a source of the systematic uncertainty of the EGB. The instrumental background from mis-classified CRs also contributes to the error of the EGB spectrum. To overcome this issue, Ref. 31) adopted very stringent event selection criteria at the expense of efficiency. The Galactic diffuse gamma-ray emission was modeled using the GALPROP code, with particular attention given to characterizing the systematic uncertainties in the foreground modeling. The isotropic background was then derived through a simultaneous fit to the Galactic diffuse emission, resolved gamma-ray sources and the solar gamma-ray emission in $|b| \geq 10°$. The obtained isotropic component contained the contributions from the CR background. The residual background was estimated using the detailed instrument simulation, and then sub-

tracted from the fitted isotropic component to obtain the true EGB. The derived EGB spectrum from 200 MeV to 100 GeV is shown in Figure 3 (left), which visually shows how important the modeling of the Galactic diffuse emission is to evaluate the EGB spectrum.

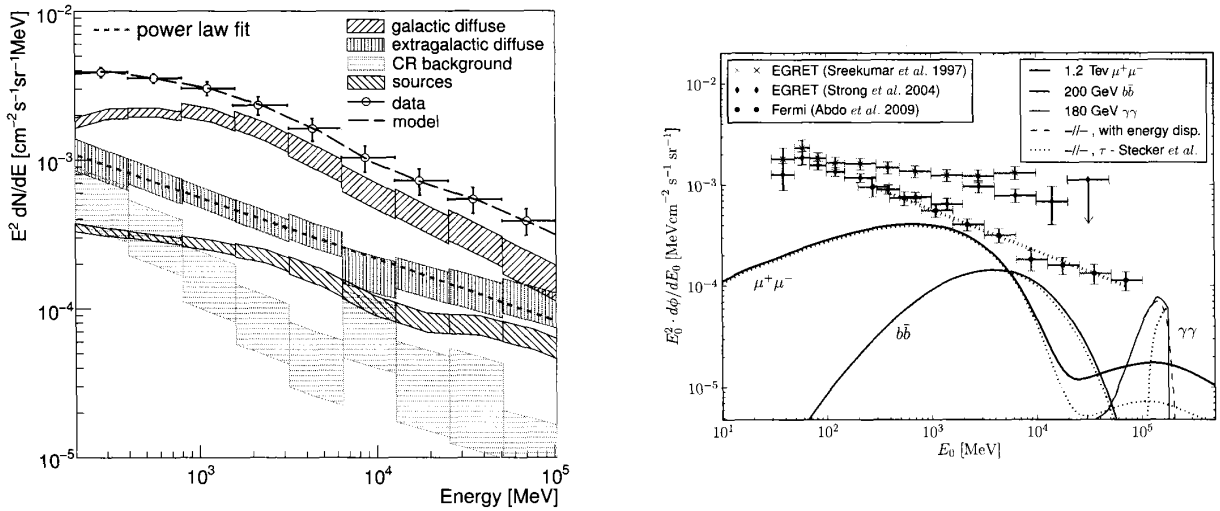

Fig. 3. (left) *Fermi*-LAT measured gamma-ray intensity with fit results for the energy range from 200 MeV to 100 GeV and for $|b| \geq 10^{\circ}$ reported by Ref. 31). Note that LAT data are dominated by the systematic uncertainties, not the statistical errors. (right) Extragalactic gamma-ray background spectra measured by *Fermi*-LAT and EGRET, together with three potential types of gamma-ray spectra induced by dark matter considered in the analysis of Ref. 32).

Using the *Fermi*-LAT EGB, Ref. 32) consider three types of generic dark matter candidates with distinctively different gamma-ray signatures: those annihilating into quarks, charged leptons and monochromatic photons. The most conservative limit on an annihilation cross section $\langle \sigma v \rangle$ can be placed by restricting the dark matter signals not to exceed the measured intensity. Predicted gamma-ray fluxes from annihilating dark matter are strongly affected by the underlying distribution of dark matter, and a moderate case considered by Ref. 32) for three representative annihilation final states ($\mu^+\mu^-$, $b\bar{b}$, and $\gamma\gamma$) is exemplified by Figure 3 right panel. The obtained limits for the dark matter cross sections are $\langle \sigma v \rangle = 1.2 \times 10^{-23}$ cm^{3}s^{-1} (for a 1.2 TeV WIMP annihilating to $\mu^+\mu^-$), 5×10^{-25} cm^{3}s^{-1} (for a 200 GeV WIMP annihilating to $b\bar{b}$) and 2.5×10^{-26} cm^{3}s^{-1} (for a 180 GeV WIMP annihilating to $\gamma\gamma$). It is already possible for leptonic dark matter model to exclude some model space proposed to explain the excess of electrons and positrons measured by the *Fermi*-LAT and PAMELA experiments. (See also § 4)

The limits obtained so far were a factor of 10–1000 times higher than the expected thermal WIMP cross section, $\langle \sigma v \rangle \sim 3 \times 10^{-26}$ cm^{3}s^{-1}. More stringent limit can be derived in principle by first subtracting the contributions from unresolved astrophysical sources. Ref. 33) examined the log$N$-log$S$ distribution of high-latitude sources. They found that most of unassociated high-latitude sources are likely to be blazars (see Figure 4 left panel). The distribution is compatible at brighter fluxes (more than 6×10^{-8} ph cm^{-2} s$-$1) with a Euclidean function, but at fainter fluxes the log$N$-log$S$ distribution displays a significant flattening. By extrapolating and integrating the log$N$-log$S$ distribution to zero flux, they derived a fraction of less than 40% for the contribution by blazars to the EGB, as summarized by Figure 4 right panel. The contribution of other sources is less determined but has been extensively studied by theoretical calculations (e.g., Ref. 34),35)).

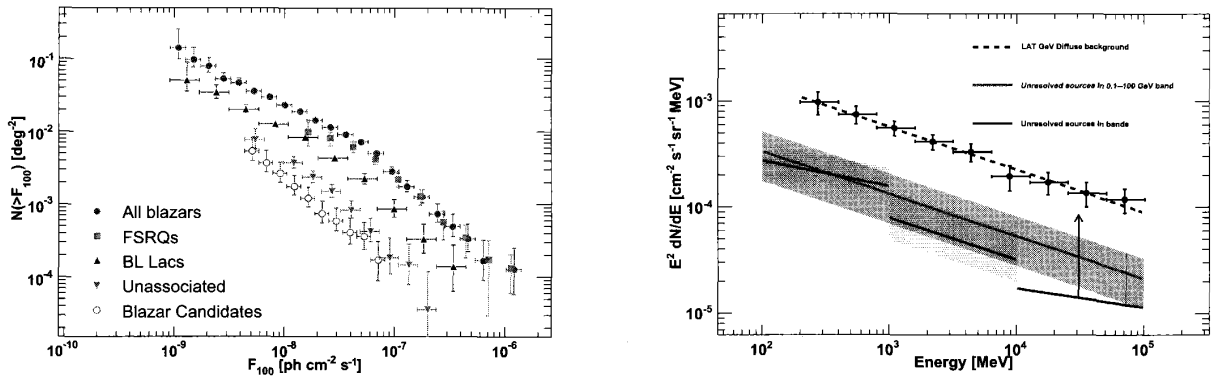

Fig. 4. (left) Cumulative source count distribution of *Fermi* blazars and subsamples reported by Ref. 33). (right) Contribution of point sources to the EGB obtained by extrapolating and integrating the log$N$-log$S$ to zero flux, taken from Ref. 33). The line from 100 MeV to 100 GeV was derived from the study of log$N$-log$S$ in the whole band, while three solid lines come from the study of individual energy band. The bands show the total (statistical and systematic) uncertainty.

§4. Cormic-Ray Electrons

It was recognized in the early stage of the LAT design that being a pair-conversion type gamma-ray telescope, the LAT intrinsically is an electron spectrometer.[36] Thanks to its large effective erea, large solid angle and long exposure, the LAT gives by far the highest statistics on CR electron and positron spectrum from about 10 MeV to 1 TeV.

The resulting spectrum of high energy CR electrons from 7 GeV to 1 TeV is shown in Figure 5 (left) together with the CR electron spectra previously reported. The *Fermi*-LAT spectrum smoothly connects with the HESS electron measurements at higher energies and can be fitted by a power-law with spectral index of 3.03–3.13 within the systematic errors. It does not confirm the anomalous spectral features reported by ATIC.[16]

Nevertheless, there is a less dramatic feature apparent above 200 GeV in the *Fermi*-LAT spectrum. While the data are compatible with a power-law spectrum within the systematic uncertainties, if a model with a power-law spectrum constrained by other data (such as the model curve shown in the figure) is compared with the *Fermi*-LAT data, the significance of the spectral feature can be high. Therefore the *Fermi*-LAT data and the positron fraction measured by PAMELA[15] have motivated the construction of dark matter models to produce the apparent features observed by these instruments. Those scenarios require a self-annihilation cross section about 100-1000 times larger than the expected thermal WIMP cross section ($\langle\sigma v\rangle \sim 3 \times 10^{-26}$ cm^{3}s^{-1}) to explain the relatively large number of additional electrons and positrons, as discussed, e.g., by Ref. 18). Some parameter space of such models is excluded by the *Fermi*-LAT EGB spectrum.[32]

A more conservative scenario is to invoke the nearby CR electron/positron accelerators such as pulsars. If a few sources are responsible of PAMELA positron fraction and *Fermi*-LAT electron spectrum, anisotropy of CR electron may be observed in high energies. Although *Fermi*-LAT has not detected significant anisotropy of the arrival direction in 60 GeV up to 480 GeV, the obtained upper limit has been already close to the expectations from individual nearby pulsars, as shown by Figure 5 (right).

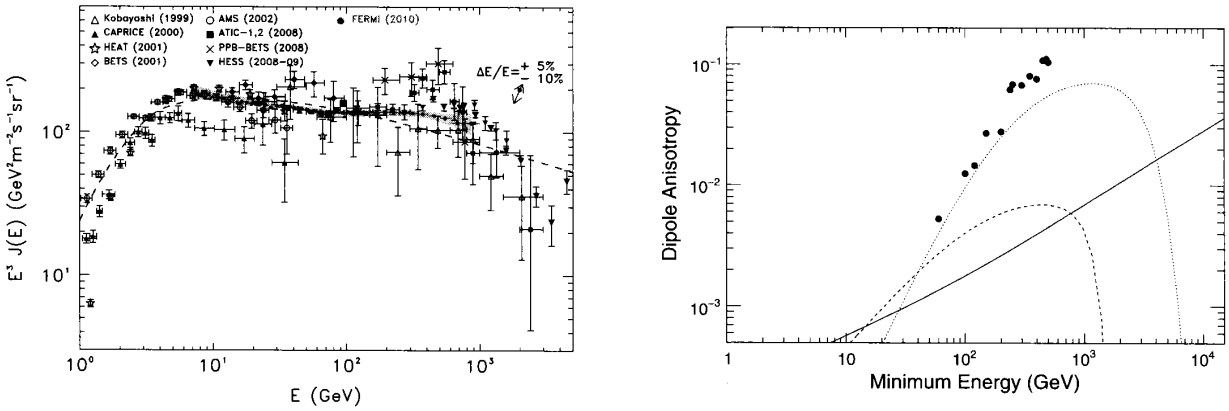

Fig. 5. (left) The *Fermi*-LAT CR electron spectrum compared with previous measurements.[37] The band shows systematic errors. Dashed line shows the model based on pre-*Fermi* results. (right) Dipole anisotropy as a function of minimum energy of *Fermi*-LAT CR electrons reported by Ref. 38). Solid line corresponds to the pure diffusive model calculated by GALPROP. The anisotropy expected from two nearby pulsars are shown by dashed and dotted lines. See Ref. 38) for details.

Acknowledgements

The *Fermi* LAT Collaboration acknowledges support from a number of agencies and institutes for both development and the operation of the LAT as well as scientific data analysis. These include NASA and DOE in the United States, CEA/Irfu and IN2P3/CNRS in France, ASI and INFN in Italy, MEXT, KEK, and JAXA in Japan, and the K. A. Wallenberg Foundation, the Swedish Research Council and the National Space Board in Sweden. Additional support from INAF in Italy and CNES in France for science analysis during the operations phase is also gratefully acknowledged.

References

1) Kraushaar, W. L., et al., Astrophys. J. **188** (1972), 341
2) Fichtel C. E., et al., Astrophys. J. **222** (1978), 833
3) Lebrun F., et al., A&A **107** (1982), 390
4) Hunter, S. D., et al., Astrophys. J. **481** (1997), 205
5) Strong, A. W., et al., Astrophys. J. **537** (2000), 763
6) de Boer W., et al., A&A **444** (2005), 51
7) Strong, A. W., et al., Astrophys. J. **613** (2004), 962
8) Atwood, W. B., et al., Astrophys. J. **697** (2009), 1071
9) Fichtel, C. E., et al., Astrophys. J. **198** (1975), 163
10) Sreekumar, P., et al., Astrophys. J. **494** (1998), 523
11) Stecker, F. W., & Salamon M. H. Astrophys. J. **464** (1996), 600
12) Chiang, J., & Mukherfee, R. Astrophys. J. **496** (1998), 752
13) Mücke, A., & Pohl, M. MNRAS **312** (2000), 177
14) Loeb, A., & Waxman, E. Nature **405** (2000), 156
15) Adriani, O., et al., Nature **458** (2009), 607
16) Chang, J., et al., Nature **456** (2008), 362
17) Aharonian, F. A., et al., Phys. Rev. Lett. **101** (2008), 261104
18) Grasso, D., et al., Astroparticle Physics **32** (2009), 140
19) Abdo, A. A., et al., Phys. Rev. Lett. **103** (2009), 251101
20) Lebrun, F., et al., Astrophys. J. **274** (1983), 231
21) Kalberla, P. M. W., et al., A&A **440** (2005), 775
22) Tibaldo, L., et al., Nuovo Cimento C., **34** 3 (2010), 163
23) Abdo, A. A., et al., Astrophys. J. **710** (2010), 133

24) Ackermann, M., et al., Astrophys. J. **726** (2011), 81
25) Strong, A. W., et al., A&A **207** (1988), 1
26) Bloemen, H., ARA&A **27** (1989), 469
27) Stecker, F. W. et al, Astrophys. J. **217** (1977), 843
28) Evoli, C. et al., JCAP **10** (2008), 18
29) Breitschwerdt, D., et al., A&A **385** (2002), 216
30) Baltz, E. A., et al., JCAP **7** (2008), 13
31) Abdo, A. A., et al., Phys. Rev. Lett. **104** (2010), 101101
32) Abdo, A. A., et al., JCAP **1004** (2010), 14
33) Abdo, A. A., et al., Astrophys. J. **720** (2010), 435
34) Fields, B. D., et al., Astrophys. J. **722** (2010), L199
35) Makiya, R., et al., Astrophys. J. **728** (2011), 158
36) Moiseev, A., et al., Proc. of XXX ICRC **2** (2007), 449
37) Ackermann, M., et al., Phys. Rev. D **82** (2010), 092004
38) Ackermann, M., et al., Phys. Rev. D **82** (2010), 092003